

Communication

## Cytochrome P450-Catalyzed Hydroxylation Initiating Ether Formation in Platensimycin Biosynthesis

Jeffrey D. Rudolf, Liao-Bin Dong, Xiao Zhang, Hans Renata, and Ben Shen

*J. Am. Chem. Soc.*, **Just Accepted Manuscript** • Publication Date (Web): 14 Sep 2018

Downloaded from <http://pubs.acs.org> on September 14, 2018

### Just Accepted

“Just Accepted” manuscripts have been peer-reviewed and accepted for publication. They are posted online prior to technical editing, formatting for publication and author proofing. The American Chemical Society provides “Just Accepted” as a service to the research community to expedite the dissemination of scientific material as soon as possible after acceptance. “Just Accepted” manuscripts appear in full in PDF format accompanied by an HTML abstract. “Just Accepted” manuscripts have been fully peer reviewed, but should not be considered the official version of record. They are citable by the Digital Object Identifier (DOI®). “Just Accepted” is an optional service offered to authors. Therefore, the “Just Accepted” Web site may not include all articles that will be published in the journal. After a manuscript is technically edited and formatted, it will be removed from the “Just Accepted” Web site and published as an ASAP article. Note that technical editing may introduce minor changes to the manuscript text and/or graphics which could affect content, and all legal disclaimers and ethical guidelines that apply to the journal pertain. ACS cannot be held responsible for errors or consequences arising from the use of information contained in these “Just Accepted” manuscripts.

# Cytochrome P450-Catalyzed Hydroxylation Initiating Ether Formation in Platensimycin Biosynthesis

Jeffrey D. Rudolf<sup>1</sup>, Liao-Bin Dong<sup>1</sup>, Xiao Zhang<sup>1</sup>, Hans Renata<sup>1</sup>, and Ben Shen<sup>1,2,3\*</sup>

<sup>1</sup>Department of Chemistry, The Scripps Research Institute, Jupiter, FL 33458, USA; <sup>2</sup>Department of Molecular Medicine, The Scripps Research Institute, Jupiter, FL 33458, USA; and <sup>3</sup>Natural Products Library Initiative at The Scripps Research Institute, The Scripps Research Institute, Jupiter, FL 33458, USA

Supporting Information Placeholder

**ABSTRACT:** Platensimycin (PTM) and platencin (PTN) are potent and selective inhibitors of bacterial and mammalian fatty acid synthases. The regio- and stereospecificity of the ether oxygen atom in PTM, which PTN does not have, strongly contribute to the selectivity and potency of PTM. We previously reported the biosynthetic origin of the 11*S*,16*S*-ether moiety by characterizing the diterpene synthase PtmT3 as a (16*R*)-*ent*-kauran-16-ol synthase and isolating 11-deoxy-16*R*-hydroxylated congeners of PTM from the  $\Delta$ *ptmO5* mutant. PtmO5, a cytochrome P450, was proposed to catalyze formation of the ether moiety in PTM. Here we report the *in vitro* characterization of PtmO5, revealing that PtmO5 stereoselectively hydroxylates the C-11 position of the *ent*-kaurane scaffold resulting in an 11*S*,16*R*-diol intermediate. The ether moiety, the oxygen of which originates from the P450-catalyzed hydroxylation at C-11, is formed via cyclization of the diol intermediate. This study provides mechanistic insight into ether formation in natural product biosynthetic pathways.

Platensimycin (PTM) and platencin (PTN) are potent and selective inhibitors of bacterial and mammalian fatty acid synthases and are promising drug leads for both antibacterial and antidiabetic therapies.<sup>1</sup> PTM shows ~1000-fold selectivity for the chain-elongation condensing enzyme FabF/FabB over the chain-initiation condensing enzyme FabH;<sup>2</sup> PTN dually inhibits FabF/FabB and FabH.<sup>3</sup> The differences in target selectivity between these two natural products is a result of their structural variations. PTM and PTN are both composed of two distinct scaffolds, an aliphatic ketolide moiety and a 3-amino-2,4-dihydroxybenzoic acid, connected by a propionamide linker (Figures 1A and S1A).<sup>2,3</sup> The ketolides of PTM and PTN are highly processed moieties originating from the diterpene scaffolds *ent*-kauranol and *ent*-atiserene, respectively.<sup>1,4</sup> Unlike PTN, the ketolide of PTM possesses an 11*S*,16*S*-tetrahydrofuran ring (Figure 1A), which hydrogen bonds

to a Thr residue in FabF and strongly contributes to the selectivity and potency of PTM.<sup>2</sup> The 11*S* configuration of this oxygen is also critical as evidenced by the 128-fold decrease in antibacterial activity of 11-deoxy-16*R*-hydroxy-PTM (Figure S1A).<sup>5</sup>

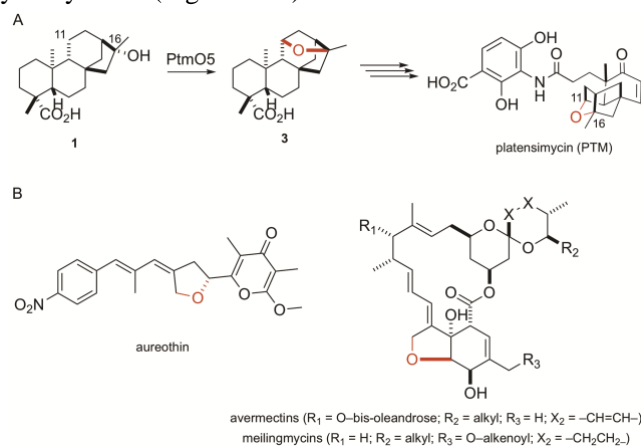


**Figure 1.** Ether formation by P450s in the biosynthesis of platensimycin, aureothin, and the avermectins and meilingmycins. (A) PtmO5-catalyzed ether formation in the biosynthesis of platensimycin was proposed based on *in vivo* gene inactivation studies.<sup>5</sup> (B) Structures of aureothin, the avermectins, and the meilingmycins, each of which contains a tetrahydrofuran ring where ether formation was proposed to be catalyzed by a P450.

We previously cloned and sequenced the *ptm* and *ptn* biosynthetic gene clusters,<sup>4,6</sup> revealing the presence of a five-gene (*ptmO3*, *ptmO4*, *ptmT3*, *ptmO5*, and *ptmR3*) cassette in the middle of the *ptm* gene cluster and suggesting that this PTM cassette encodes the genes necessary for the divergence between PTM and PTN biosynthesis, i.e., the construction of the tetrahydrofuran-containing *ent*-kaurane skeleton (Figure S1B). We subsequently reported the biosynthetic origin of the 11*S*,16*S*-ether moiety by characterizing PtmT3 as a (16*R*)-*ent*-kauran-16-ol synthase (Figure S1C) and isolating eight PTM congeners from the  $\Delta$ *ptmO5* mutant.<sup>5</sup> Each of the congeners lacked the tetrahydrofuran ring and instead featured an 11-deoxy-16*R*-hydroxylated diterpene

scaffold. These data led us to propose that PtmO5, a cytochrome P450, catalyzes ether formation in PTM biosynthesis.<sup>5</sup>

To test the mechanism of ether formation in PTM biosynthesis, we cloned *ptmO5* from *S. platensis* CB00739<sup>6</sup> and heterologously produced PtmO5 in *E. coli* (Tables S1–S3 and Figure S2A). We found that the putidaredoxin reductase CamA and putidaredoxin CamB from the P450<sub>cam</sub> system are capable redox partners for PtmO5 (Figure S2A).<sup>7</sup> PtmO5, which exists as a monomer in solution (Figure S2B), was first confirmed as

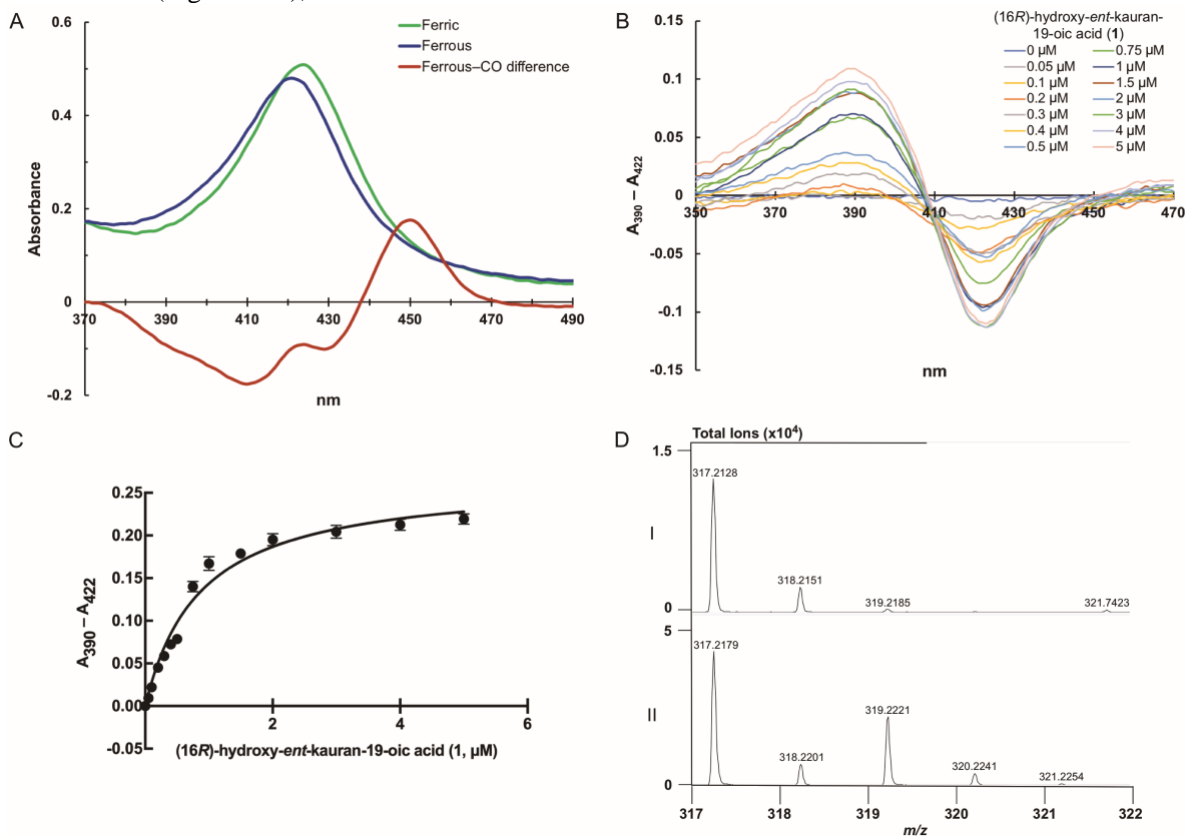


**Figure 2.** Biochemical characterization of PtmO5. (A) The ferrous–CO difference spectrum of PtmO5 yielded an absorbance maximum at 450 nm. (B) Type I binding spectra resulting from titration of PtmO5 with **1** (0–5 μM). (C) Determination of the  $K_d$  for **1** based on nonlinear regression of the absorption differences ( $A_{390}-A_{422}$ ) in the type I difference spectra versus the concentration of **1**. (D) HRESIMS of product **3** after quenching the reaction mixture of PtmO5 and **1** with acid, supporting the ether oxygen originates from molecular oxygen. (I) Reaction performed in air resulted in an  $[M+2-H]^-/[M-H]^-$  ion ratio of 0.023; (II) reaction performed in the presence of  $^{18}\text{O}_2$  resulted in an increase of the  $[M+2-H]^-$  ion and an  $[M+2-H]^-/[M-H]^-$  ion ratio of 0.512.

When PtmO5 was incubated with **1** in the presence of CamA, CamB, and NADH, one new enzymatic product (**2**) was found after the reaction mixture was analyzed by LC-MS in comparison with that of the boiled enzyme control (Figure 3A). The polar product had an  $[M-H]^-$  ion at  $m/z$  335.2256 (Figure S3), supporting a molecular formula of  $\text{C}_{20}\text{H}_{32}\text{O}_4$  (calculated  $[M-H]^-$  ion at  $m/z$  335.2228) and consistent with that of a hydroxylated analogue of **1**; surprisingly, the expected ether-containing product, (11*S*,16*S*)-*ent*-kauran-11,16-epoxy-19-oic acid (**3**), was not detected. Product **2** was enzymatically prepared, isolated, and characterized by 1D and 2D NMR

an authentic P450 based on the observance of a Soret band at 450 nm in the ferrous–CO versus ferrous difference spectrum (Figure 2A). When PtmO5 was incubated with its presumptive substrate (16*R*)-hydroxy-*ent*-kauran-19-oic acid (**1**), a characteristic type I binding spectrum was observed resulting in a  $\lambda_{\text{max}}$  shift from 422 nm to 390 nm (Figure 2B). Using increasing concentrations of **1**, we determined a dissociation constant ( $K_d$ ) of  $0.86 \pm 0.07 \mu\text{M}$  for the complex of PtmO5–**1** (Figure 2C).

spectroscopy (Table S4 and Figures S4–S9). Based on the NMR data, the only difference between **2** and **1** was the presence of a hydroxyl group at C-11 ( $\delta_{\text{C}}$  66.8;  $\delta_{\text{H}}$  3.88, d,  $J = 7.0 \text{ Hz}$ ) in **2**. HMBC correlations between H-11 and C-9 ( $\delta_{\text{C}}$  66.4), C-10 ( $\delta_{\text{C}}$  39.9), and C-13 ( $\delta_{\text{C}}$  49.6), as well as COSY correlations between H-11 and H-9 ( $\delta_{\text{H}}$  1.19) and H-11 and H<sub>2</sub>-12 ( $\delta_{\text{H}}$  1.96, 1.76), also supported the assignment of the hydroxyl group at C-11 (Figure S10). Based on the ROESY correlations of H-11 with H<sub>3</sub>-20 ( $\delta_{\text{H}}$  0.88) and H-11 with H-1a ( $\delta_{\text{H}}$  1.92), the hydroxyl group at C-11 was assigned the 11*S* configuration (Figures 3B and S10). Although this chemical structure was recently

reported,<sup>8</sup> our NMR data had significant differences (~10 ppm) in the chemical shifts for C-9, C-12, and C-14

(Table S4), suggesting a different structural isomer for the previously reported natural product.

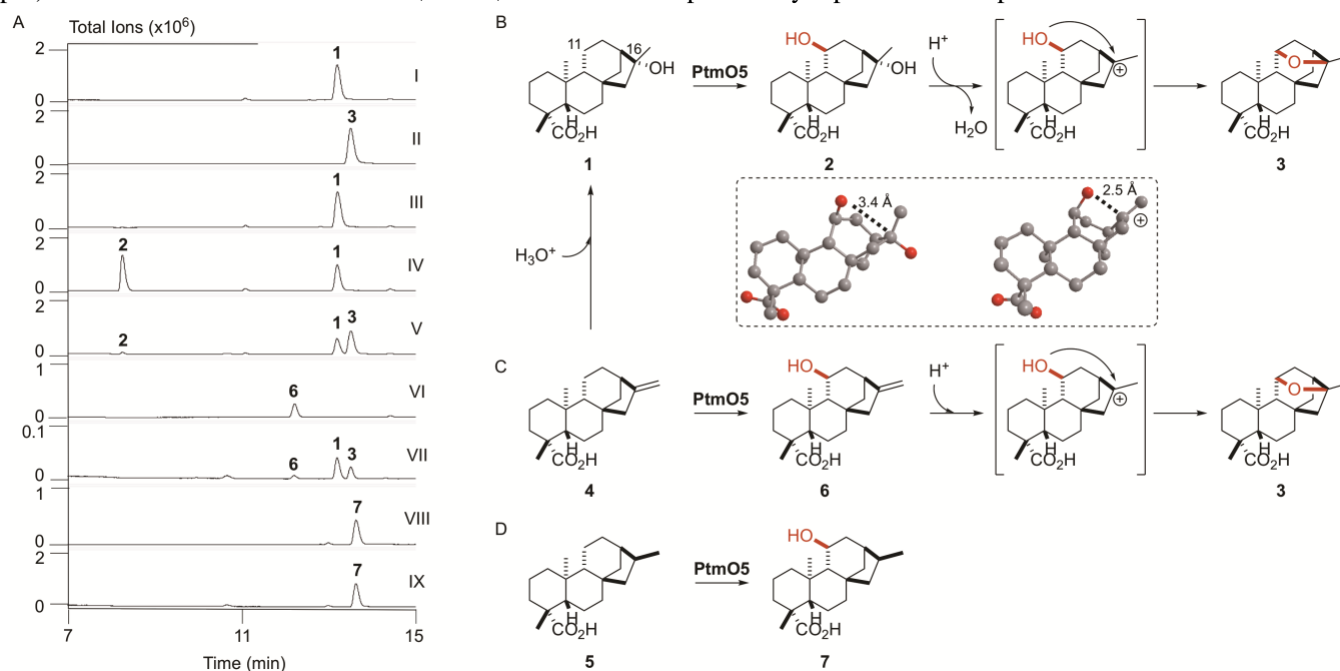


**Figure 3.** Ether formation in PTM biosynthesis proceeds through 11*S*-hydroxylation of **1** by PtmO5 followed by cyclization of the diol intermediate. (A) Total ion chromatograms (TICs) of PtmO5 reactions. All reactions were incubated with CamA, CamB, and NADH. (I) **1** std; (II) **3** std; (III) **1** incubated with boiled PtmO5; (IV) **1** incubated with PtmO5; (V) acid-quenched reaction with **1**; (VI) **4** incubated with PtmO5; (VII) acid-quenched reaction with **4**; (VIII) **5** incubated with PtmO5; (IX) acid-quenched reaction with **5**. Substrates **4** and **5** were undetectable by LC-MS. (B) In vitro, PtmO5 catalyzes the 11*S*-hydroxylation of **1** to form diol **2**, which undergoes acid-mediated ether formation to yield **3**. Distances between C-16 and O-11 of **2** and the (11*S*)-hydroxy-*ent*-kauran-19-oic acid cation (inset) were determined using ChemDraw 3D (MM2 energy-minimized). Loss of water at C-16 results in a conformational change that decreases the distance between O-11 and C-16. (C) PtmO5 catalyzes the 11*S*-hydroxylation of **4** to form **6**, which also undergoes acid-mediated ether formation to yield **3**. Upon acid quenching, **4** forms **1**. (D) PtmO5 catalyzes the 11*S*-hydroxylation of **5** to form **7**, which cannot undergo acid-mediated ether formation.

Since **3** was not detected in the PtmO5 reaction, we tested if incubation of PtmO5 with diol **2** facilitated enzymatic ether formation. However, when PtmO5 was incubated with **2** in the presence of CamA, CamB, and NADH, no new enzymatic products were detected (Figure S11).

Since ether formation was not seen in the PtmO5 reaction, we proposed that a nonenzymatic intramolecular nucleophilic substitution reaction could generate the ether bond. Given the tertiary alcohol at C-16, we suspected that acid may facilitate ether formation via an S<sub>N</sub>1 mechanism. Protonation of the alcohol and subsequent loss of a water molecule would generate a tertiary carbocation at C-16, which could be easily quenched by the oxygen at C-11 (Figure 3B). Carbocation generation at C-16 would also result in a conformational change of the terpene skeleton, thereby decreasing the distance between C-16 and O-11 from 3.4 Å to 2.5 Å (Figure 3B). Indeed, when the PtmO5 reaction with **1** was quenched with acid (final pH ~2), a new product, with a molecular weight and retention time consistent with that of **3**, was found by LC-MS analysis (Figure 3A). Performing the PtmO5 reaction in buffers with pH values ranging from

5–9 (not acid quenched) revealed that lower pH values did not facilitate the formation of **3**, while negatively affecting the efficiency of hydroxylation (Figure S12).

The inversion of stereochemistry at C-16 during ether formation in PTM biosynthesis, i.e., 16*R* in **1** to 16*S* in **3** and thus in PTM (Figure 1A), requires the oxygen installed by PtmO5 to close the tetrahydrofuran ring. To confirm that the ether oxygen is derived from molecular oxygen, **1** was incubated with PtmO5 in the presence of <sup>18</sup>O<sub>2</sub>. Analysis of the acid-quenched reaction mixture by LC-MS revealed a substantial increase in the [M – H]<sup>–</sup> ion at *m/z* 319.2221 (Figure 2D), corresponding to the <sup>18</sup>O-labeled ether product **3**. Therefore, the ether oxygen in PTM originates from the P450-catalyzed hydroxylation of C-11.

To further support a possible nonenzymatic S<sub>N</sub>1 mechanism for ether formation in PTM biosynthesis, we individually incubated *ent*-kaur-16-en-19-oic acid (**4**) and chemically synthesized (16*S*)-*ent*-kauran-19-oic acid (**5**) (Scheme S1, Figure 3CD) with PtmO5. Type I binding spectra were observed for both **4** and **5**, yielding K<sub>d</sub> values of 0.75 ± 0.19 μM and 1.5 ± 0.2 μM, respectively (Figure S13). LC-MS analysis of the respective enzyme reactions

revealed that PtmO5 hydroxylated both **4** and **5**, yielding the enzymatic products **6** and **7**, respectively (Figure 3CD). Due to poor solubility of **4**, we were unable to isolate enough **6** to determine its structure by NMR. However, when the reaction with **4** was quenched with acid, two new peaks, **1** and **3**, were detected (Figure 3A). The formation of **3** likely occurs through a similar nucleophilic mechanism where the 11S-hydroxyl group would quench the C-16 tertiary carbocation formed by acid-catalyzed protonation of the double bond (Figure 3C).<sup>9</sup> Protonation and nonenzymatic water quench of **4** yields **1** (Figure 3C).<sup>10</sup>

Product **7** was enzymatically prepared, isolated, and characterized by HRESIMS, and 1D and 2D NMR spectroscopy (Table S4 and Figures S14–S21). Similar to **2**, **7** clearly possessed an 11S-hydroxyl group, which was further supported by HMBC and ROESY correlations (Figures 3D and S10). As expected, **3** was not formed when acid was added to the reaction mixture containing **5** and **7** (Figure 3A). Together, these data provide evidence that PtmO5 hydroxylates the C-11 position of the *ent*-kauranol scaffold resulting in a diol intermediate that might undergo nonenzymatic ether formation. Although ether formation was realized in vitro under strong acidic conditions, it may not be relevant in vivo. We cannot rule out the possibility that PtmO5, or another enzyme from the *ptm* gene cluster, catalyzes ether formation in vivo. If another enzyme is needed, it would likely require a strong acidic environment for protonation, such as the anti-configured Asp in *ent*-copalyl diphosphate synthase and squalene-hopene synthase.<sup>11</sup>

Nature utilizes several different strategies to catalyze oxidative cyclizations in natural product biosynthesis.<sup>12</sup> P450s, which are widely-known to form C–O bonds, are capable of forming cyclic ether bonds.<sup>13</sup> In *Streptomyces*, AurH, AveE, and MeiE, have been implicated in the formation of tetrahydrofuran rings in the biosynthesis of aureothin, avermectin, and meilingmycin, respectively (Figure 1B).<sup>14–17</sup> It is still unclear whether these cyclic ethers are formed via two hydroxylations and subsequent dehydration, or sequential hydroxylation, hydrogen abstraction, and diradical combination (Figure S22AB).

Ether formation in PTM biosynthesis is inherently different from those in aureothin, avermectin, and meilingmycin biosynthesis. The C-16 tertiary alcohol in **1** allows facile carbocation generation and nucleophilic attack by the C-11 hydroxyl group. The lack of a tertiary alcohol prevents acid-mediated cyclization, as evidenced by the absence of tetrahydrofuran formation of synthetically prepared (7*R*)-7,9a-dihydroxy-deoxyaureothin in the presence of acid.<sup>18</sup> Thus, the ethers generated by AurH, AveE, and MeiE likely do not follow a similar cationic-driven ether formation mechanism. It should be noted that a few terpene synthases, such as 1,8-cineole synthase and corvol ether synthase, can directly

form ether bonds through a similar cationic and intramolecular quenching mechanism.<sup>19</sup>

Assuming that nonenzymatic ether formation is an actual physiological process, the nature of ether formation in PTM suggests that other ether bonds in natural products biosynthesis may be formed in a similar manner. For example, AtmQ from paspalicine biosynthesis, which is proposed to form a 1,3-dioxolane ring between two tertiary alcohols,<sup>20</sup> likely follows a similar mechanism to that of PtmO5 (Figure S22C). The tetrahydrofuran ring in aspterric acid also likely undergoes sequential P450 hydroxylation and spontaneous ether formation; albeit occurring by nucleophilic attack of an epoxide (Figure S22D).<sup>21</sup>

In summary, we characterized PtmO5 as a P450 that is involved in ether formation in the biosynthesis of PTM. PtmO5 regio- and stereoselectively hydroxylates the C-11 position resulting in an 11*S*,16*R*-diol intermediate that undergoes ether formation via cyclization. This study showcases how the structural complexity of natural product scaffolds, in addition to the vast diversity of enzymes, contributes towards the generation of biologically relevant functional groups in natural products.

## ASSOCIATED CONTENT

**Supporting Information.** Materials and methods. Strains, plasmids, and primers used in this study (Tables S1–S3); summary of NMR data for compounds **2** and **7** (Table S4); structures, biosynthetic gene clusters, and proposed biosynthetic pathway of PTM and PTN (Figure S1); SDS-PAGE analysis and size exclusion chromatography of PtmO5 (Figure S2); HRESIMS and NMR spectra of **2** (Figures S3–S9); key 2D NMR correlations of **2** and **7** (Figure S10); LC-MS chromatograms of the PtmO5 enzyme reaction with **2** (Figure S11); LC-MS chromatograms of the PtmO5 enzyme reactions in buffers with varying pH values (Figure S12); type I binding spectra and  $K_d$  determinations for **4** and **5** (Figure S13); HRESIMS of **6** (Figure S14); HRESIMS and NMR spectra of **7** (Figures S15–S21); proposed mechanisms of ether formation in aureothin, meilingmycin, paspalicine and aspterric acid biosynthesis (Figure S22); NMR spectra of **4**, **8**, and **5** (Figures S23–S25). The Supporting Information is available free of charge on the ACS Publications website.

## AUTHOR INFORMATION

### Corresponding Author

\*[shenb@scripps.edu](mailto:shenb@scripps.edu).

### Funding Sources

No competing financial interests have been declared. This work is supported in part by the National Institutes of Health Grant GM114353 (B.S.) and GM128895 (H.R.). J.D.R. is supported in part by a National Institutes of Health Pathway to Independence Award GM124461.

## ACKNOWLEDGMENTS

We thank Dr. Jian-Jun Chen of the State Key Laboratory of Applied Organic Chemistry, College of Chemistry and Chemical Engineering, Lanzhou University for a standard of *ent*-kaur-16-en-19-oic acid. This is manuscript #29727 from The Scripps Research Institute.

## REFERENCES

1. Rudolf, J. D.; Dong, L.-B.; Shen, B., Platensimycin and platencin: Inspirations for chemistry, biology, enzymology, and medicine. *Biochem. Pharm.* **2017**, *133*, 139-151.
2. Wang, J.; Soisson, S. M.; Young, K.; Shoop, W.; Kodali, S.; Galgoci, A.; Painter, R.; Parthasarathy, G.; Tang, Y. S.; Cummings, R.; Ha, S.; Dorso, K.; Motyl, M.; Jayasuriya, H.; Ondeyka, J.; Herath, K.; Zhang, C.; Hernandez, L.; Allocco, J.; Basilio, A.; Tormo, J. R.; Genilloud, O.; Vicente, F.; Pelaez, F.; Colwell, L.; Lee, S. H.; Michael, B.; Felcetto, T.; Gill, C.; Silver, L. L.; Hermes, J. D.; Bartizal, K.; Barrett, J.; Schmatz, D.; Becker, J. W.; Cully, D.; Singh, S. B., Platensimycin is a selective FabF inhibitor with potent antibiotic properties. *Nature* **2006**, *441* (7091), 358-361.
3. Wang, J.; Kodali, S.; Lee, S. H.; Galgoci, A.; Painter, R.; Dorso, K.; Racine, F.; Motyl, M.; Hernandez, L.; Tinney, E.; Colletti, S. L.; Herath, K.; Cummings, R.; Salazar, O.; Gonzalez, I.; Basilio, A.; Vicente, F.; Genilloud, O.; Pelaez, F.; Jayasuriya, H.; Young, K.; Cully, D. F.; Singh, S. B., Discovery of platencin, a dual FabF and FabH inhibitor with in vivo antibiotic properties. *Proc. Natl. Acad. Sci. U. S. A.* **2007**, *104* (18), 7612-7616.
4. Smanski, M. J.; Yu, Z.; Casper, J.; Lin, S.; Peterson, R. M.; Chen, Y.; Wendt-Pienkowski, E.; Rajski, S. R.; Shen, B., Dedicated *ent*-kaurene and *ent*-atiserene synthases for platensimycin and platencin biosynthesis. *Proc. Natl. Acad. Sci. U. S. A.* **2011**, *108* (33), 13498-13503.
5. Rudolf, J. D.; Dong, L.-B.; Manoogian, K.; Shen, B., Biosynthetic origin of the ether ring in platensimycin. *J. Am. Chem. Soc.* **2016**, *138* (51), 16711-16721.
6. Hindra; Huang, T.; Yang, D.; Rudolf, J. D.; Xie, P.; Xie, G.; Teng, Q.; Lohman, J. R.; Zhu, X.; Huang, Y.; Zhao, L.-X.; Jiang, Y.; Duan, Y.; Shen, B., Strain prioritization for natural product discovery by a high-throughput real-time PCR method. *J. Nat. Prod.* **2014**, *77* (10), 2296-2303.
7. Peterson, J. A.; Lorence, M. C.; Amarneh, B., Putidaredoxin reductase and putidaredoxin. Cloning, sequence determination, and heterologous expression of the proteins. *J. Biol. Chem.* **1990**, *265* (11), 6066-73.
8. Ma, X.-H.; Wang, Z.-B.; Zhang, L.; Li, W.; Deng, C.-M.; Zhong, T.-H.; Li, G.-Y.; Zheng, W.-M.; Zhang, Y.-H., Diterpenoids from *Wedelia prostrata* and their derivatives and cytotoxic activities. *Chem. Biodiversity* **2017**, *14* (5), e1600423.
9. Herz, W.; Sharma, R. P., New hydroxylated *ent*-kauranoic acids from *Eupatorium album*. *J. Org. Chem.* **1976**, *41* (6), 1021-1026.
10. Cavalcanti, B. C.; Bezerra, D. P.; Magalhaes, H. I. F.; Moraes, M. O.; Lima, M. A. S.; Silveira, E. R.; Caamara, C. A. G.; Rao, V. S.; Pessoa, C.; Costa-Lotufo, L. V., Kauren-19-oic acid induces DNA damage followed by apoptosis in human leukemia cells. *J. Appl. Toxicol.* **2009**, *29* (7), 560-568.
11. Köksal, M.; Hu, H.; Coates, R. M.; Peters, R. J.; Christianson, D. W., Structure and mechanism of the diterpene cyclase *ent*-copalyl diphosphate synthase. *Nat. Chem. Biol.* **2011**, *7* (7), 431-433.
12. Tang, M.-C.; Zou, Y.; Watanabe, K.; Walsh, C. T.; Tang, Y., Oxidative cyclization in natural product biosynthesis. *Chem. Rev.* **2017**, *117* (8), 5226-5333.
13. Rudolf, J. D.; Chang, C.-Y.; Ma, M.; Shen, B., Cytochromes P450 for natural product biosynthesis in *Streptomyces*: sequence, structure, and function. *Nat. Prod. Rep.* **2017**, *34* (9), 1141-1172.
14. He, J.; Mueller, M.; Hertweck, C., Formation of the aureothin tetrahydrofuran ring by a bifunctional cytochrome P450 monooxygenase. *J. Am. Chem. Soc.* **2004**, *126* (51), 16742-16743.
15. Richter, M. E. A.; Traitcheva, N.; Knuepfer, U.; Hertweck, C., Sequential asymmetric polyketide heterocyclization catalyzed by a single cytochrome P450 monooxygenase (AurH). *Angew. Chem., Int. Ed.* **2008**, *47* (46), 8872-8875.
16. Pang, C.-H.; Matsuzaki, K.; Ikeda, H.; Tanaka, H.; Omura, S., Production of 6,9a-seco-6,8a-deoxy derivatives of avermectins by a mutant strain of *Streptomyces avermitilis*. *J. Antibiot.* **1995**, *48* (1), 59-66.
17. He, Y.; Sun, Y.; Liu, T.; Zhou, X.; Bai, L.; Deng, Z., Cloning of separate meilingmycin biosynthesis gene clusters by use of acyltransferase-ketoreductase didomain PCR amplification. *Appl. Environ. Microbiol.* **2010**, *76* (10), 3283-3292.
18. Henrot, M.; Jean, A.; Peixoto, P. A.; Maddaluno, J.; De Paolis, M., Flexible total synthesis of ( $\pm$ )-aureothin, a potent antiproliferative agent. *J. Org. Chem.* **2016**, *81* (12), 5190-5201.
19. Dickschat, J. S., Bacterial terpene cyclases. *Nat. Prod. Rep.* **2016**, *33* (1), 87-110.
20. Zhang, X.; Li, S., Expansion of chemical space for natural products by uncommon P450 reactions. *Nat. Prod. Rep.* **2017**, *34* (9), 1061-1089.
21. Yan, Y.; Liu, Q.; Zang, X.; Yuan, S.; Bat-Erdene, U.; Nguyen, C.; Gan, J.; Zhou, J.; Jacobsen, S. E.; Tang, Y., Resistance-gene-directed discovery of a natural-product herbicide with a new mode of action. *Nature* **2018**, *559* (7714), 415-418.

Insert Table of Contents artwork here

